

# AN EXPERIMENTAL STUDY ON FLOW CHARACTERISTICS OF A LIQUID FILM FALLING ON A VERTICAL COLUMN OF HORIZONTAL TUBES

**Gherhardt Ribatski**

Heat and Mass Transfer Laboratory (LTCM)  
École Polytechnique Fédérale de Lausanne (EPFL)  
ME GO 560, Station 9  
CH-1015 Lausanne, Switzerland  
gherhardt.ribatski@epfl.ch

**Abstract.** A visual study is presented of a liquid film falling on a vertical row of horizontal plain tubes. Experiments were performed for water and ethylene glycol using different liquid supply arrangements. The effects of film flow rate and tube size and spacing on the liquid film distribution were investigated. Measurements of sheet contraction and of droplet and column departure-site spacing were obtained. Pronounced sheet contractions were observed, reaching up to 2/3 of the initial sheet length. The reduction of the film length was also found to be substantial for the column and droplet intertube flow modes. Droplet and column departure-site spacing increased with tube diameter. For ethylene glycol, droplet and column departure-site spacing increased slightly with tube row depth. An negligible effect was noticed for water. The obtained results are thoroughly discussed with regard to the physical and operational control parameters for falling-film flows.

**Keywords.** Two-Phase Flow; Falling-Film; Horizontal Tubes; Heat Exchangers; Flow Pattern.

## 1. Introduction

Falling film evaporators with bundles of horizontal tubes can be found on a wide array of thermal and chemical system applications. Generally speaking, they are attractive principally because they provide a high heat transfer coefficient and operate with low fluid inventory. Such characteristics result in some advantages for falling film evaporators over flood tube bundles, viz. potential reduction in the heat exchanger size and lower risks associated with a leak. In addition, the pressure drop through the falling film evaporator is almost negligible. However, according to a comprehensive state of the art review on falling film evaporation on horizontal tubes presented by Ribatski and Jacobi (2005), the thermal performance of the falling-film heat exchanger may be drastically affected by the distribution of the fluid refrigerant along the tube bundle according to the following aspects: (1) flow mode between adjacent surfaces; (2) flow unsteadiness; (3) film thickness along the heating surfaces; (4) flow contraction along the tube bundle, and consequent decrease of the wetted surface area; (5) spacing of droplet and column departure sites; (6) “slinging” effect, Wei and Jacobi (2002).

When a liquid film flows from one horizontal tube to another below it, the flow may take the form of droplets, circular columns, or a continuous sheet. Extensive studies focusing on characterization and prediction of flow modes were performed by Armbruster and Mitrovic (1994) and Hu and Jacobi (1996), both studies on plain tubes, and recently by Roques *et al.* (2002) on plain and enhanced tubes. The flow modes identified by Hu and Jacobi (1996) are shown in Fig. 1. By comparing the current prediction methods for flow mode transitions, Ribatski and Jacobi (2005) found a significant scatter among them, which is reasonable given the subjective nature of interpreting two-phase flow regimes. It must to be noted, however, that not one of these previous studies investigated the effect of the bundle depth on flow mode transitions.

For the droplet and column flow modes, liquid usually falls from fix sites along the underside of the tube. The distance between them,  $\lambda$ , seems to be related to the Taylor instability. For circumstances in which viscous effects are negligible and the fluid is incompressible, Bellman and Pennington (1954) found that the critical wavelength, and most dangerous Taylor wavelength are given respectively by:

$$\lambda_c = 2\pi \cdot \sqrt{\frac{\sigma}{g \cdot (\rho_l - \rho_v)}}; \quad \lambda_D = \lambda_c \cdot \sqrt{3} \quad (1)$$

where  $\rho_l$  and  $\rho_v$  are the liquid and vapor densities, respectively,  $\sigma$  is the surface tension and  $g$  is the gravitational acceleration.

Only perturbations having wavelengths between  $\lambda_c$  and  $\lambda_D$  will grow. However,  $\lambda_D$  is the wavelength for which the disturbance grows most rapidly. Therefore, in real systems, the dominant disturbance wavelength is generally close to  $\lambda_D$ .

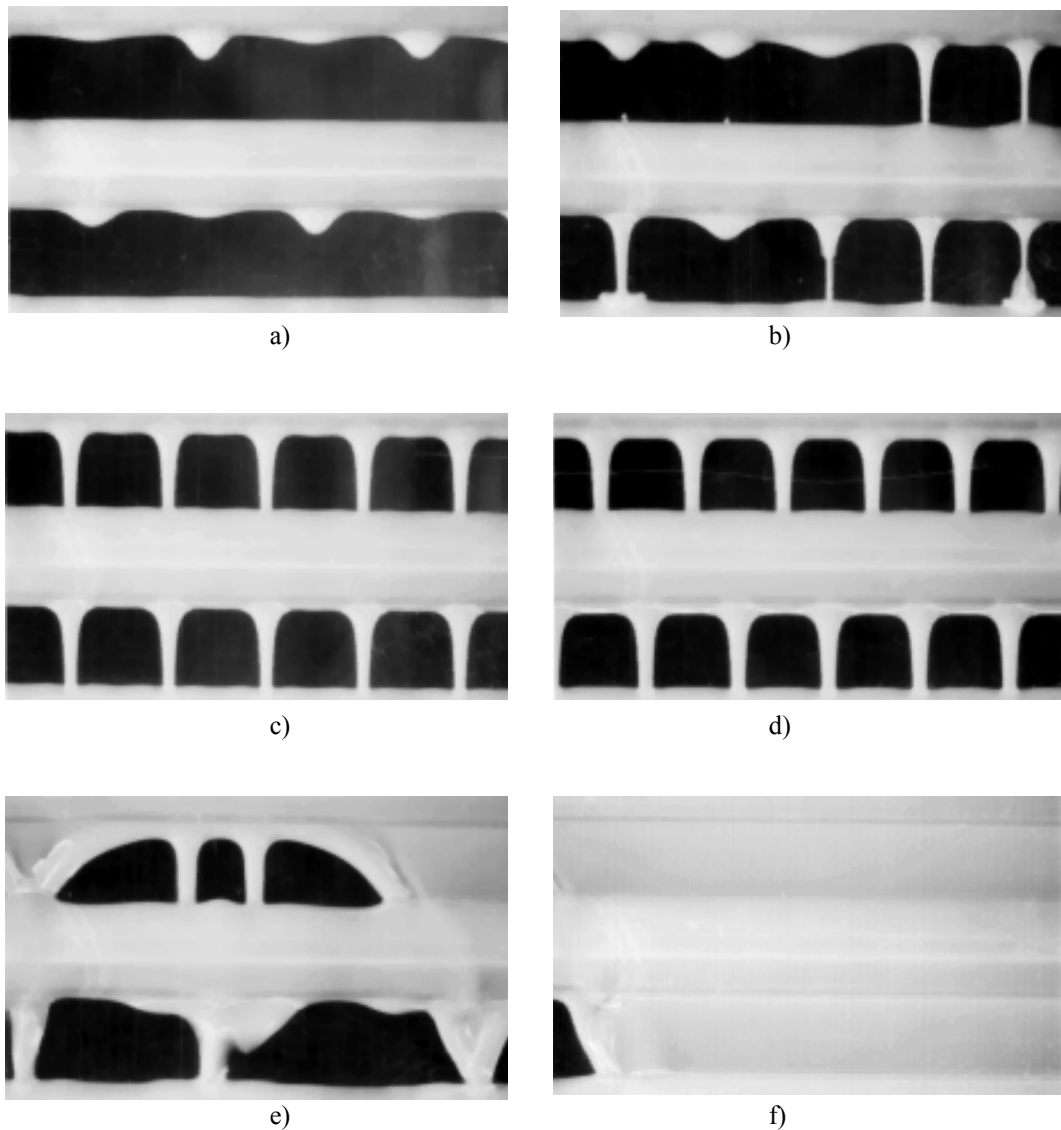


Figure 1. Intertube flow modes for ethylene glycol according to Hu and Jacobi (1996). (a) droplet; (b) droplet-column; (c) in-line column; (d) staggered column; (e) column-sheet; (f) sheet mode.

Yung *et al.* (1980) performed an experimental study with water, ethylene glycol and ammonia, and concluded that  $\lambda$  is given by  $\lambda_c \cdot \sqrt{2}$ . For the column mode and water as working fluid, Ganić and Roppo (1980) concluded that the film flow rate, the intertube distance, and the fin spacing do not affect  $\lambda$ , whose value was generally lower than  $\lambda_c$  given by Eq. (1). Departure-site spacing being unaffected by the geometrical characteristics of the tube fins was also observed by Roque *et al.* (2002) on Turbo-BII, Turbo-Chil, and Thermoexcel tubes. They performed experiments using water, ethylene glycol, and a 50 percent water/50 percent ethylene glycol as working fluids. Mitrovic (1986) found departure-site spacing values between the critical and the most dangerous wavelength. He pointed out values of 22mm for water at 25°C and of 13.5mm for alcohol at 21.5°C. Honda *et al.* (1987) conducted experiments involving condensation on low finned tubes using R-113, methanol, and normal propanol. They reported values of  $\lambda$  close to  $\lambda_c$  in the column mode, and lower than  $\lambda_c$  in the droplet mode.

Armbruster and Mitrovic (1994) suggested that the effects of physical properties on column spacing are adequately described by the capillary constant given by:

$$a = \sqrt{\frac{\sigma}{g(\rho_l - \rho_v)}} \quad (2)$$

In addition, they found that  $\lambda$  decreases slightly with increasing the film flow rate. More recently, Armbruster and Mitrovic (1995) correlated the column spacing as

$$\lambda = \frac{2\pi\sqrt{2}}{\sqrt{a^{-2} \left[ 1 + \left( Re/Ga^{1/4} \right)^{0.8} \right] + 2/D^2}} \quad (3)$$

where  $D$  is the tube diameter,  $Re$  is the film Reynolds number given by  $Re=4\Gamma/\mu_l$  and  $Ga$  is the modified Galileo number given by  $Ga=\rho_l\sigma^3/\mu_l^4g$ .  $\Gamma$  is the liquid mass flow rate per unit length of tube (each side) and  $\mu_l$  is the liquid dynamic viscosity. This correlation is based on data from water and isopropyl alcohol, and described their experimental results within  $\pm 7.5\%$ .

An extensive analysis of the departure-site spacing on droplet and column modes was made by Hu and Jacobi (1998). Their experiments covered a wide range of tube diameters and tube pitches, being performed with water, ethylene glycol, a water-glycol mixture, and hydraulic oil. They found that a decrease in the flow rate is accompanied by an increase in  $\lambda$ , and the degree at which  $\Gamma$  affects  $\lambda$  was greater at low  $\Gamma$  (droplet mode). They suggested that as  $Re \rightarrow 0$ , the droplet departure-site spacing seems to approach  $\lambda_D$  given by Eq. (1). Tube diameter effects were greater at small diameters, and  $\lambda$  increased with the tube diameter. Except at  $(s-D)/a \approx 5$ , the condition in which  $\lambda$  presented a minimum, a weak dependence on the tube pitch  $s$  was noted. Preliminary results suggested that a concurrent air flow decreases  $\lambda$ . Hu and Jacobi (1998) also presented a qualitative study on liquid-column shapes and a correlation according to which  $\lambda$  is given by:

$$\frac{\lambda}{a} = \frac{0.836A - 0.836(Re/Ga^{1/4})}{\left[ 1 + \left( \frac{0.836A - 0.836(Re/Ga^{1/4})}{0.75A - (85/Ga^{1/4})} \right)^2 \right]^{1/2}} \quad \text{where} \quad A = \frac{2\pi\sqrt{3}}{\sqrt{1 + 2(a/D)^2}} \quad (4)$$

Recently, Habert *et al.* (2006) performed intercolumn spacing measurements for R236fa at a saturation temperature of 20°C. Results were obtained for a plain tube and two 3D enhanced condensing surfaces. They reported average distances between two successive columns of  $7.3 \pm 0.9$  mm for the plain tube and of  $8.4 \pm 0.9$  mm and  $7.6 \pm 0.7$  mm for the structured tubes within a 95% confidence interval. These values lie between the critical wavelength  $\lambda_c$  and the most dangerous Taylor wavelengths  $\lambda_D$ , which are 5.6 mm and 9.7 mm for R236fa at 20°C, respectively.

According to the review of the pertinent literature, aspects related to the effects of the bundle-depth on the film flow mode, column/droplet spacing and flow contraction are still unclear. Thus, in the present paper, an experimental investigation was conducted to observe a liquid film falling on a vertical row of five horizontal plain tubes. The first part of the paper is dedicated to the description of the experimental set-up and procedure. In the second part, the experimental results are described and it is presented a thorough discussion on the effects of the film flow rate, tube spacing, tube diameter, working fluid, hysteresis (differences in the flow behavior while increasing or reducing the film flow rate), and bundle-depth on the flow contraction, film flow mode between adjacent surfaces, and column/droplet spacing. Then, comparisons of the measured experimental  $\lambda$  against current prediction are reported.

## 2. Experimental Apparatus and Procedure

The experimental set-up and the test section are shown schematically in Figs. 2 and 3, respectively. The test set-up consists of a closed-circuit, forced-circulation loop of liquid. The test section was made of acrylic glass. Thus, the falling-film flow can be observed through the front plate of the test section.

A variable speed gear pump drives the working fluid through the circuit. The type of pump was chosen to keep stable the mass flow and the pressure. From the pump, the test fluid flows through a filter and the flow meter to the liquid distributor on the top of the test section. To obtain a fine adjustment of the liquid mass flow rate at the test section, a bypass needle valve was installed between the pump and the reservoir. Liquid mass flow rates are measured using a Coriolis-effect flow meter, with accuracy of  $\pm 0.1\%$  of reading. The fluid density and temperature were also measured by the flow meter with accuracies of  $\pm 2\text{kg/m}^3$  and  $\pm 1^\circ\text{C}$ , respectively. The liquid distributor described in Hu and Jacobi (1996) was designed to promote even distribution of liquid along its length.

In the test section, from the distributor, the working fluid flows around the dummy tubes and a single column of five horizontal stainless steel tubes. The dummy tubes were used to achieve a homogeneous liquid distribution along the test surfaces. After flowing around the fifth test tube the liquid falls to a receiver, returning to the reservoir as shown in Fig. 2. The dummy and test tubes were prepared by thoroughly polishing and cleaning. The tube diameter of the upper dummy tube was 7mm. The lower dummy tube has a diameter equal to the test tubes, simulating a tube row. The gaps between the distributor and the upper dummy tube, and between the dummy tubes were 1mm. Experiments were also performed with solely the upper dummy tube and without dummy tubes. It was done in order to investigate the effects of the liquid feeding method on the falling-film flow characteristics.

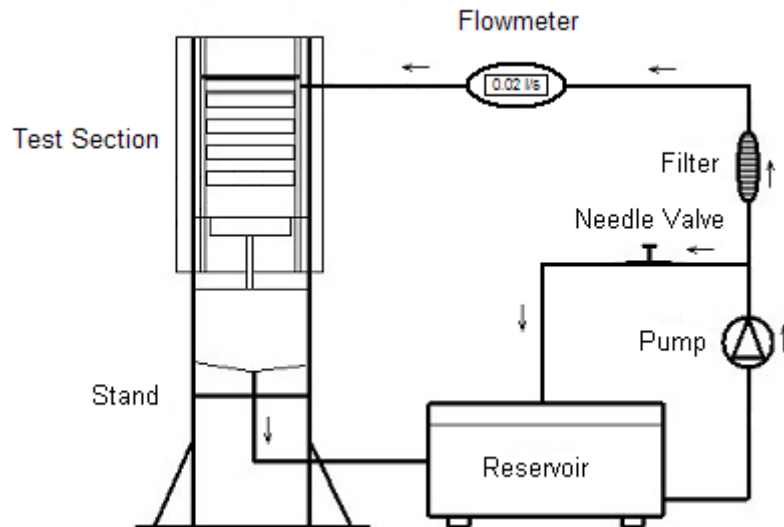


Figure 2. Schematic diagram of the experimental apparatus.

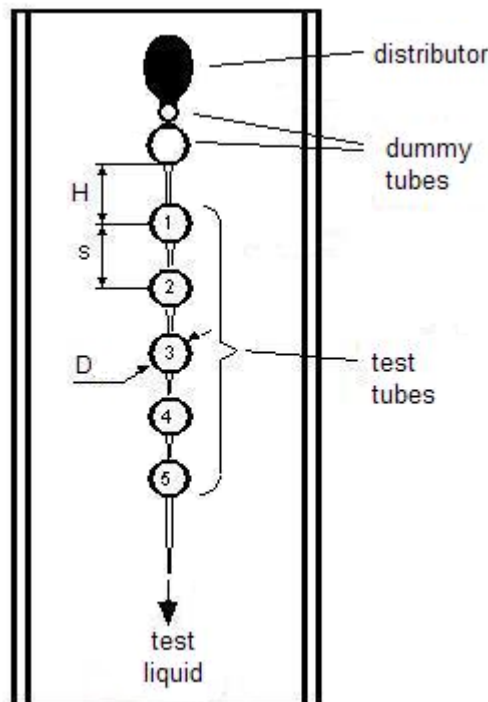


Figure 3. Schematic of the test section.

Experiments were carried out by changing tube spacing, tube diameter, working fluid and its flow rate. Care was taken on to place the tubes vertically aligned and in horizontal positions. The test liquid was circulated by several hours to ensure that the tubes were fully wetted. Tests were conducted by gradually increasing the flow rate up. Once the maximum film flow rate was attained ( $\approx 0.18 \text{ kg/ms}$ ) which in general corresponds to a value higher than the one for which the film flow mode was achieved, the flow rate was gradually reduced down to the initial value. A regular video camera was used to record the flow image and a reference image. Using commercial software, the images were digitized and the measurements performed. The uncertainty in the lengths measured from the images was  $\pm 0.5 \text{ mm}$ . Thermophysical properties were estimated according to Hu and Jacobi (1996). A fairly good amount of experimental conditions have been investigated, involving the following conditions:

- Test fluid: water and ethylene glycol;
- Liquid test temperature:  $\approx 22^\circ \text{C}$
- Mass flow rate on each side of the tube,  $\Gamma$ : up to  $0.20 \text{ kg/ms}$ ;

- Tube diameter,  $D$ : 11, 20, 40 and 80mm;
- Tube pitch,  $s$ : varying in the range between 3 and 80mm;
- Distance between the lower dummy tube and the center of the upper test surface,  $H$ : varying in the range between 8.5 and 156mm. When  $H$  is not mentioned its values corresponds to the presented tube pitch subtracted of  $D/2$ .

### 3. Results and discussion

#### 3.1. Spacing of droplet and column departure sites

For the intertube flow modes including columns and droplets, the liquid tends to detach from the lower region of the upper tube from fixed points separated by  $\lambda$ . Such a distance, as above-mentioned, is related to the Taylor instabilities and presents values close to the critical Taylor wavelength. Figure 4 shows the variation of  $\lambda$  with  $\Gamma$  for data measured between the second and third tubes in the row. In this case, the displayed results were obtained by gradually decreasing the film flow rate down to zero. According to this figure, at high flow rates the effect of  $\Gamma$  on  $\lambda$  is almost negligible. This behavior was observed even at the column-sheet flow mode. For ethylene glycol, a minimum departure-site spacing can be observed at low film flow rates beyond which  $\lambda$  increases with further decreasing in the film flow rate. This behavior was maintained downwards the tube row and was not observed for the experiments conducted by gradually increasing the film flow rate up to a maximum value. Figure 5 presents pictures illustrating the departure-site spacing behavior with decreasing film flow rate. According to this figure, lower departure-site spacings are observed at the column-droplet flow mode. Such a behavior is promoted by the appearance of a droplet departure-site between two consecutive columns. Further reductions in the film flow rate promote the transition from column-droplet to droplet flow mode beyond which  $\lambda$  increases with additional decreasing in the film flow rate. For water, it can be observed in Fig. 4 that at low film flow rates  $\lambda$  increases with decreasing  $\Gamma$ , and an occurrence of a minimum value at a certain film flow rate is not observed. Lower departure-site spacings are observed for ethylene glycol. Contrary to the results of Ganić and Roppo (1980) that observed  $\lambda$  values lower than  $\lambda_c$ , according to Fig. 4, such a behavior is observed only for ethylene glycol and, in the case of water, as pointed out by Yung *et al.* (1980)  $\lambda$  presented values between  $\lambda_c$  and  $\lambda_D$ . Hu and Jacobi (1996) suggested that, when  $\Gamma$  becomes closer to 0,  $\lambda$  tends to  $\lambda_D$ . Such a behavior is not clear according to the present study as also shown in Fig. 4.

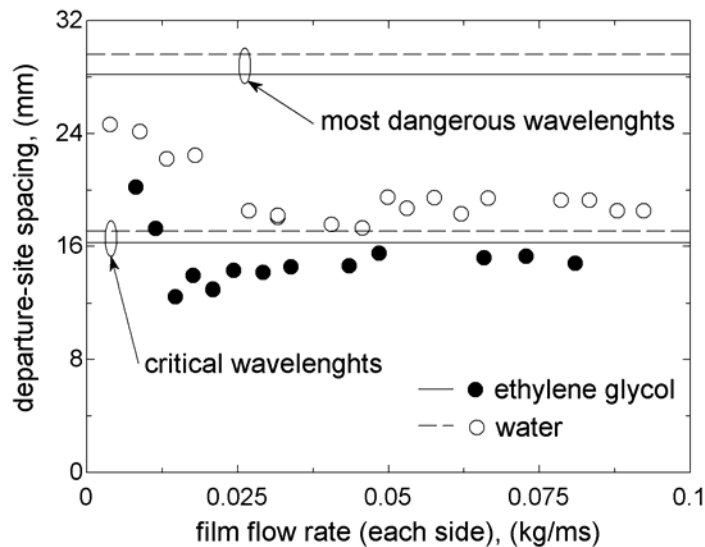


Figure 4. Illustration of the effects of the film flow rate on the departure-site spacing on the 2nd tube,  $D=11$ mm,  $H=13.5$ mm and  $s=19$ mm.

Figure 6 illustrates the effects of tube diameter and intertube spacing on the departure-site spacing. Taken into account that the departure-site spacing results presented here are average values of all measurements performed for the flow between adjacent tubes, Fig. 6 also includes bars indicating the standard deviations of these average values. Generally speaking, higher variances in  $\lambda$  were found for water, at  $\Gamma$  values near the flow-mode transitions and for experiments performed by increasing gradually the film flow rate from a minimum value. According to Fig. 6b, for an intertube distance of  $\approx 8$ mm (in red) and at film flow rates higher than 0.018kg/ms, the departure-site spacing increases with increasing tube diameter. However no clear trend is observed for an intertube distance of  $\approx 18$ mm (in blue). The fact that  $\lambda$  increases with tube diameter was observed previously by Hu and Jacobi (1996). A clear trend on the departure-site spacing with tube pitch cannot be identified in Fig. 6a. Except for  $(s-D)/a \approx 5$ , Hu and Jacobi (1996) observed a negligible effect of the tube pitch on  $\lambda$ . Similar departure-site spacing behaviors to those displayed in Fig. 6

with changing tube diameter and intertube spacing were also observed for water and for experiments performed by gradually increasing  $\Gamma$ .

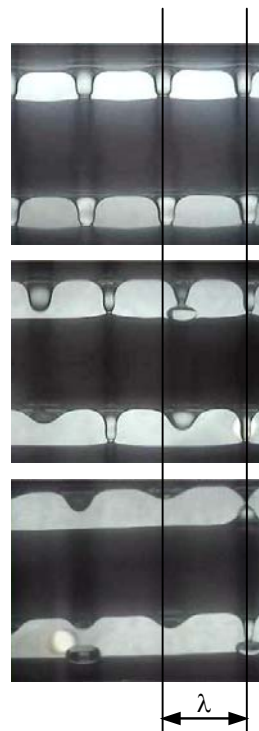


Figure 5. Pictures illustrating the variation of the departure-site spacing and flow modes with decreasing film flow rate for ethylene glycol,  $D=20\text{mm}$ ,  $s=30\text{mm}$  and  $H=34\text{mm}$ . The central tube in each picture is the 3<sup>rd</sup> test tube in the row.

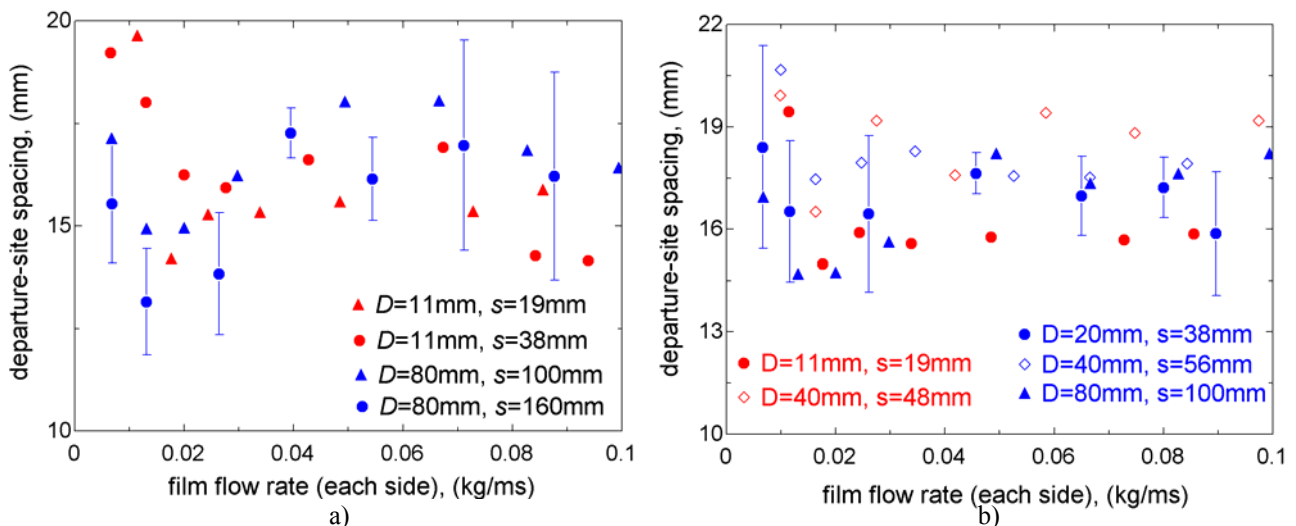


Figure 6. a) Variation of the departure-site spacing with tube pitch; b) Variation of the departure site spacing with the tube diameter for intertube distances of  $\approx 18\text{mm}$  (blue) and  $\approx 8\text{mm}$  (red). Decreasing film flow rate, ethylene glycol and measurements performed between the 3<sup>rd</sup> and 4<sup>th</sup> tubes.

Figure 7 illustrates the variation of the departure-site spacing along the tube row. For ethylene glycol, it is noted that  $\lambda$  increases downwards the tube row while for water it seems that that the position along the tube row does not affect the departure-site spacing. Higher inertial effects for water seem to be related to the fact that  $\lambda$  is kept almost constant along the tube row. Higher inertial effects are also related to the fact that for water the in-line column flow mode was rarely observed while for ethylene glycol in-line and staggered column flow modes were equally observed. By analysing the entire database, it can be concluded that the distributor, though including dummy tubes (see Fig. 3), provides lower  $\lambda$  values than those observed on the lower tubes below the distributor.

Figure 8 illustrates two distinct mechanisms related to the increase in the departure-site spacing downwards the tube row. In Fig. 8a, two impinging neighbor columns are merging during the flow on the horizontal tube resulting in only one departure site on the tube underside. Slinging effects, as those pointed out by Wei and Jacobi (2002), consisting in columns detaching from the tube row are shown in Fig. 8b. For both situations, dryout effects with a consequent decrease in the heat transfer coefficient are facilitated in the case of falling-film evaporators. In Fig. 7, as aforementioned, higher standard deviations of the average departure-site spacing for water are shown.

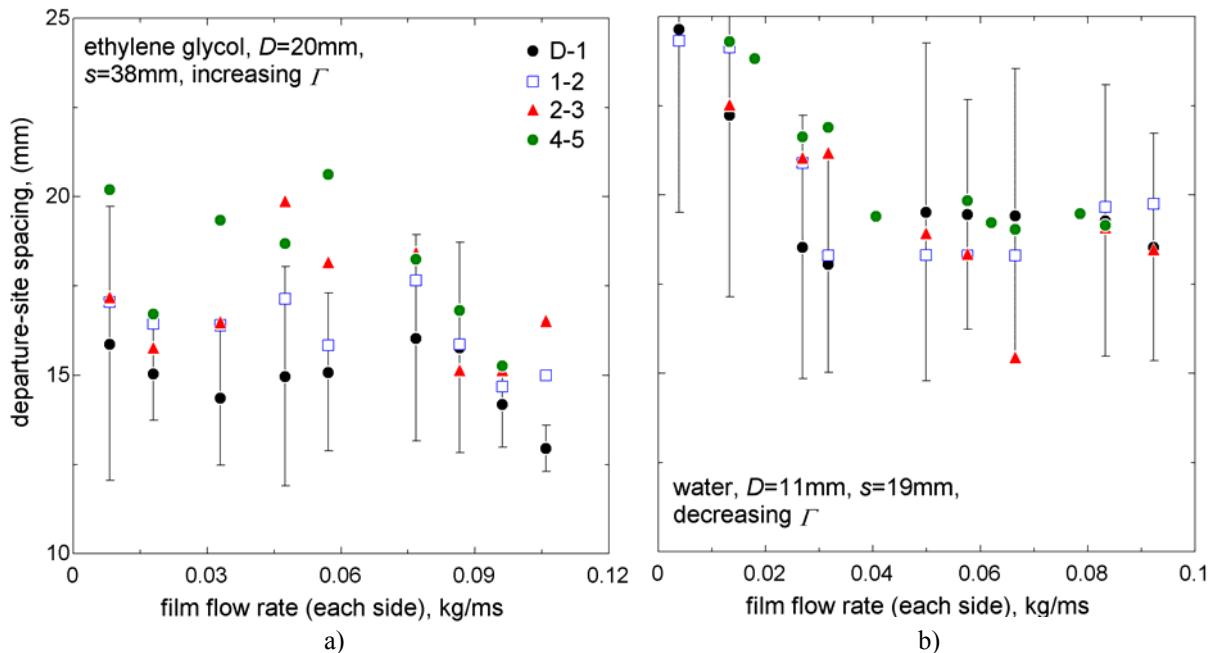


Figure 7. Illustration of the variation of the departure-site spacing downwards the tube row.

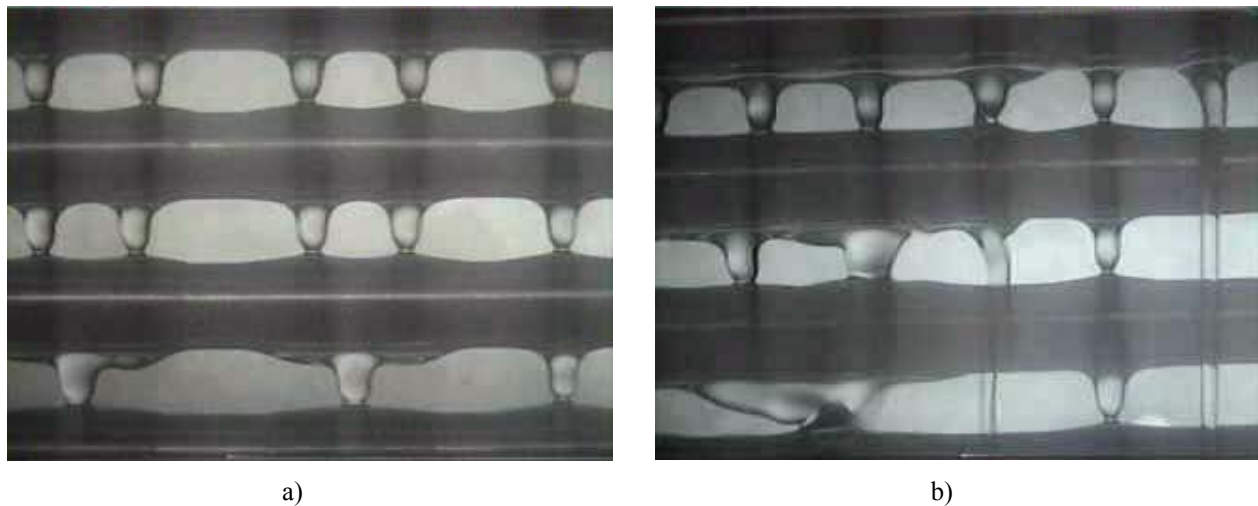


Figure 8. Pictures illustrating the following mechanism affecting  $\lambda$  along the tube row: a) merging columns, b) slinging phenomenon.

Figure 9 displays a comparison of the capability of two predictive methods from the literature plus the most dangerous Taylor wavelength to predict the present experimental departure-site spacing results. This comparison involves the entire experimental database. In this figure, the horizontal axis indicates the tubes between which the  $\lambda$  values were measured while the vertical axis give the percentage of points predicted within  $\pm 20\%$  (Fig. 9a) and  $\pm 30\%$  (Fig. 9b) of the experimental data. Generally speaking, except for the region between the distributor and the upper tube, the method proposed by Hu and Jacobi (1998) provides a better prediction. Reasonable predictions are also obtained by using the method proposed by Armbruster and Mitrovic (1994). The most dangerous Taylor wavelength predicted poorly the experimental data. Worst predictions are observed for the regions between the distributor and the upper tube

and between the fourth and fifth tubes. The liquid distributor seems to affect the liquid distribution giving lower average departure-site spacing than when the liquid distribution is a result of the liquid film flow on the horizontal tubes. Cumulative effects of instabilities and the mechanisms illustrated in Fig. 8 are related to the worst capabilities of the cited methods to predicted the inter-site spacing on the underneath of the fourth horizontal tube downwards the row.

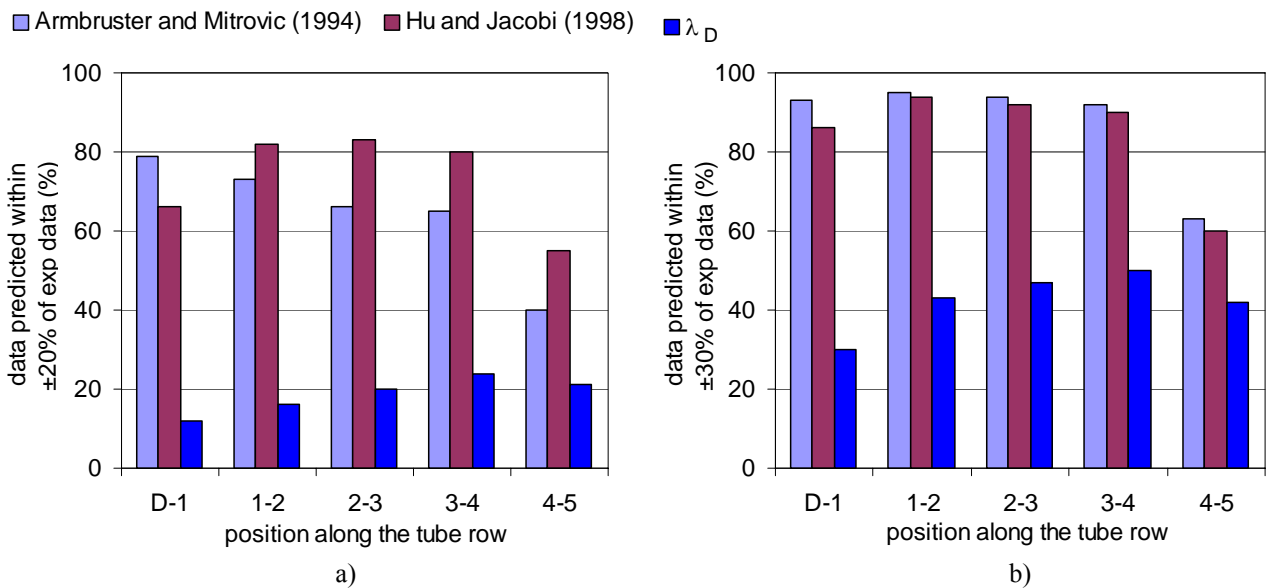


Figure 9. Comparison of the capability of the departure-site spacing predictive methods to predict the present experimental database.

### 3.2. Liquid flow contraction

The longitudinal flow contraction downward the tube row decreases the wetted surface area of the tubes. For a falling-film type evaporator, this may affect the overall heat transfer rate (i) due to a decrease in the effective heat transfer area with a consequent decrease in the overall heat transfer coefficient and also (ii) due to an increase in the liquid film thickness that, in the case of subcooled evaporation, may promote either a decrease in the heat transfer coefficient for laminar film flows or an increase in the heat transfer coefficient for turbulent film flows. According to Ribatski and Thome (2005) and Ribatski and Thome (2006), for saturated evaporation on plain tubes in the presence of boiling and non-existence of dryout conditions, the liquid film thickness does not affect the heat transfer coefficient. Based on the fact that in this study contractions of the initial longitudinal flow length higher than 40% were observed for a tube row within only 5 tubes plus the fact that the heat transfer coefficient increases smoothly with film flow rate for turbulent flows as pointed out by Ribatski and Jacobi (2005), it is concluded here that in general the longitudinal flow contraction decreases the heat exchanger performance and, thus, should be avoided.

The pictures in Fig. 10 show flow contractions at different experimental conditions. In this figure, it is revealed that longitudinal film flow contractions may occur on the horizontal tubes and also during the flow between tubes. Figure 10 reveals that although higher film flow contractions occurs at the sheet flow mode, they are also observed at the column flow mode. Superior longitudinal flow contractions were observed for each flow mode (droplet, columns and sheet) at the lowest flow rate at which the flow mode is possible as shown in Fig. 11. In general the droplet flow mode provides higher film flow contractions than the column flow mode. In Fig. 11, hysteresis effects on the film flow contraction with changing the film flow rate are also observed. Such a behavior is primarily related to hysteresis effects on the flow mode transitions. A gradual change on the film flow contraction with film flow rate close to the transition between the sheet and column flow modes is related to the existence of an intermediary flow mode (column-sheet, see Fig. 1) and the fact that, generally, the flow mode distribution at transitional film flow rates is not uniform along the tube row.

Based on Fig. 10, it can be concluded that the total film flow contraction is comprised of the following two components related to independent characteristics of the tube row: (i) contraction during the film free-fall related to the intertube distance and controlled by gravitational and surface tension effects; and (ii) contraction during the film flow on the tube that is affected by the tube diameter and controlled by inertial (related to the film free fall), viscous and surface tension effects. It is important to highlight that depending of the tube diameter and relative magnitude of the inertial effects an expansion on the film flow length can also occur during the film flow on the tubes.

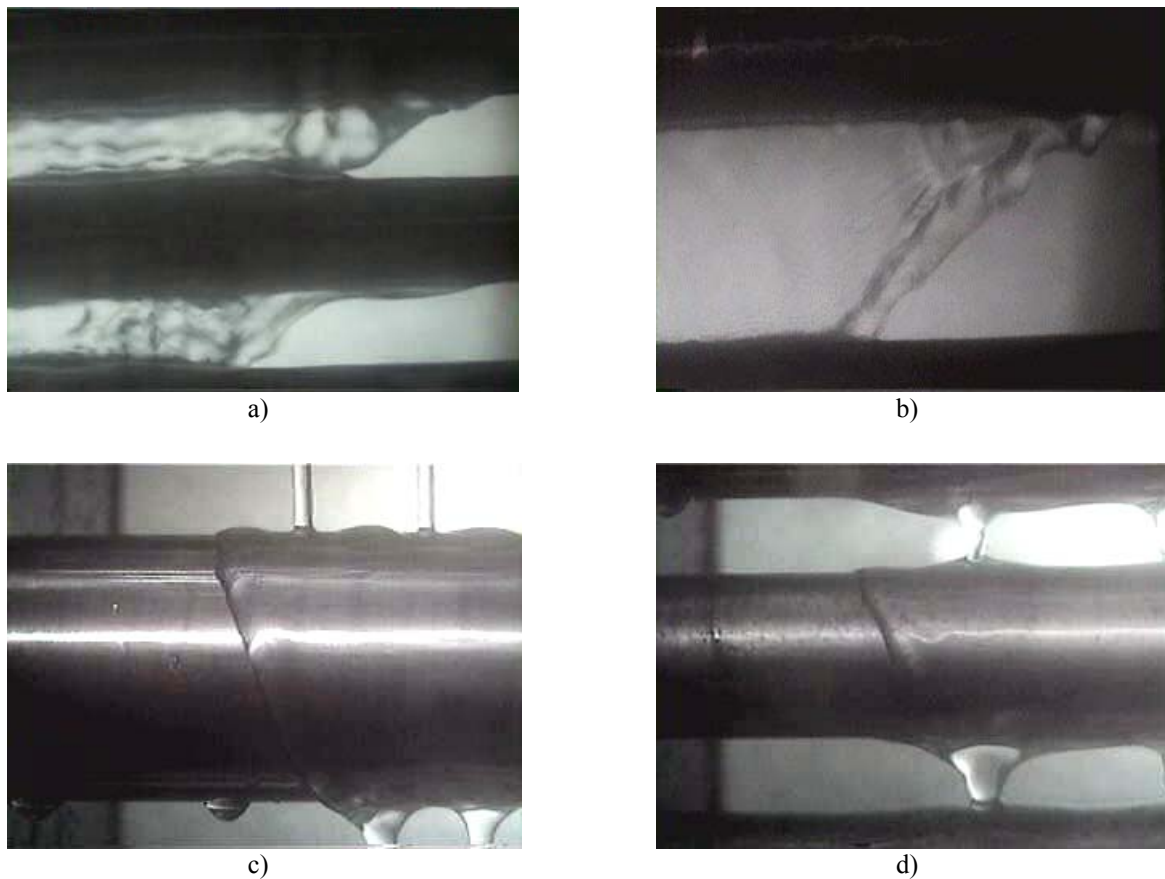


Figure 10. Pictures showing the longitudinal film flow contraction along the tube row. a) water,  $D=11$  mm,  $s=19$ mm; b) ethylene glycol,  $D=11$  mm,  $s=38$ mm; c) ethylene glycol,  $D=40$ mm,  $s=80$ mm; d) ethylene glycol,  $D=20$ mm,  $s=30$ mm.

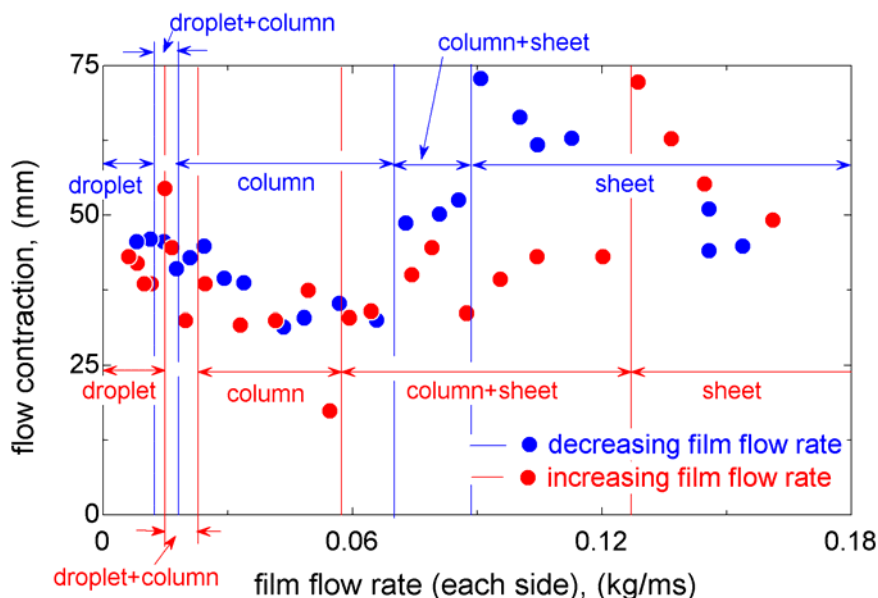


Figure 11. Illustration of the hysteresis effects on the film flow contraction (differences in the total film flow contraction behavior while increasing or reducing  $\Gamma$ ).  $D=11$  mm,  $s=19$ mm, ethylene glycol.

Figure 12 illustrates the effects of the intertube spacing and the tube diameter on the total film flow contraction. In Fig. 12a, for an intertube spacing of  $\approx 18$ mm (blue symbols) and film flow rates lower than 0.1 kg/ms, it can be noted that the total film flow contraction increases with increasing the tube diameter. A similar behavior is also observed in this figure for an intertube distance of approximately 8mm (red symbols). Superior film flow contractions on tubes having larger diameters are related to such a behavior since it was observed that the tube diameter does not affect the

intertube film flow contraction. In Fig. 12b, at higher film flow rates corresponding to the sheet flow mode, it is observed that the film flow contraction increases with increasing the tube pitch. A lower effect of the intertube distance on the total film flow contraction is displayed at the column and droplet flow modes. An increase of the film flow contraction with increasing tube spacing during the film free-fall at the sheet flow mode is related to the increase of the total flow contraction with increasing the intertube distance. At column and droplet flow modes the effect of the intertube spacing on the film flow contraction seems to be negligible. In Fig. 12b, for  $s=15\text{mm}$  and an intertube spacing of  $4\text{mm}$ , an almost constant total film flow contraction is displayed. Such a behavior seems to be related to the negligible film flow contractions during the film free-fall.

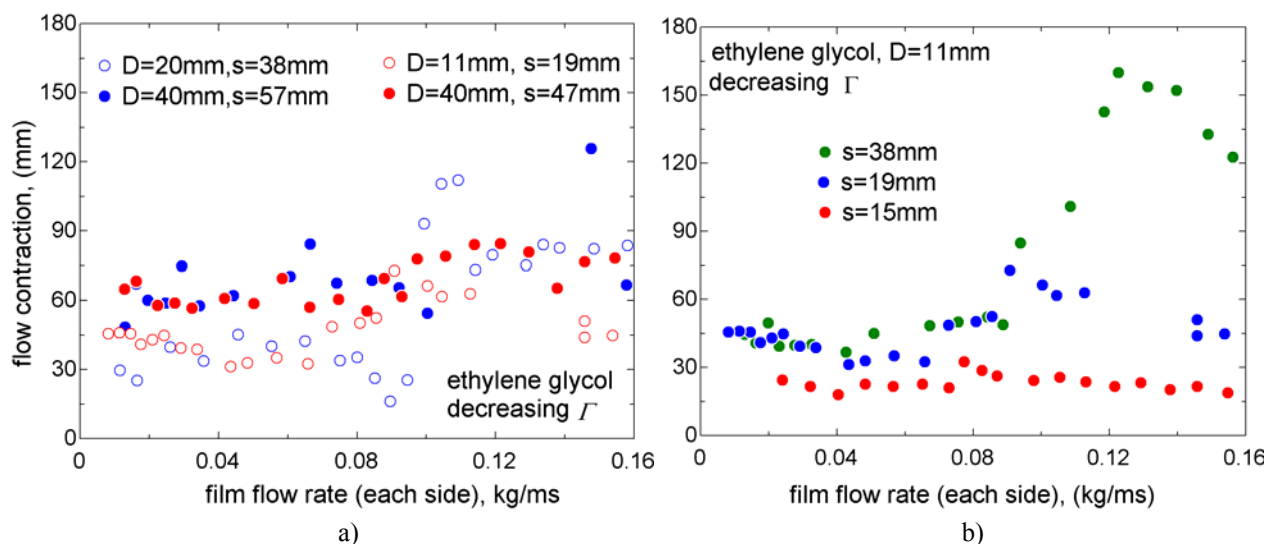


Figure 12. Illustration of the effects of (a) tube diameter and (b) the intertube spacing on the total film flow contraction.

Figure 13 illustrates the variation of the total film flow contraction with the film flow rate for water and ethylene glycol. Higher film flow contractions are displayed for ethylene glycol. In addition in this figure, an slight increase in the film flow contraction with decreasing  $\Gamma$  at the column and droplet flow modes observed for ethylene glycol is not observed for water. Through an analysis of the transport properties and the surface tension of these two fluids, clear reasons for such behaviors are not found. It can be speculated that the lower dynamic viscosity of the ethylene glycol at the same film flow rate suppresses film flow instabilities favoring surface tension effects during the intertube film flow what results in higher film flow contractions for ethylene glycol than for water.

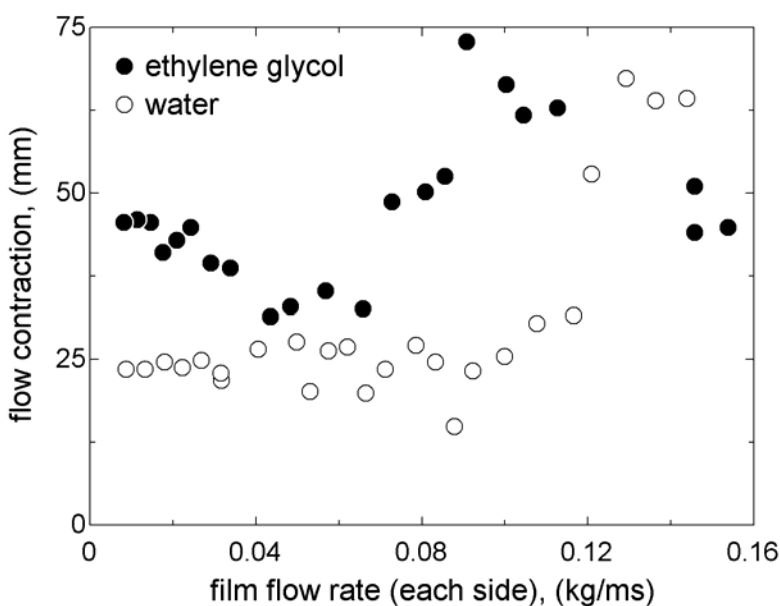


Figure 13. Illustration of the fluid type effect on the total film flow contraction for results obtained by decreasing stepwise the film flow rate,  $D=11\text{mm}$  and  $s=19\text{mm}$ .

#### **4. Conclusions**

A visual study of a liquid film falling on a vertical row of horizontal plain tubes was presented. Experiments were performed for water and ethylene glycol using different liquid supply arrangements. The effects of film flow rate and tube size and spacing on the liquid departure-site spacing and on the contraction of the longitudinal film length along the tube row were studied. Larger departure-site spacings were observed for experiments performed for water. For ethylene glycol it was found that the departure-site spacing increases downwards the tube row while for water it seems that the tube position along the row does not affect  $\lambda$ . Generally speaking, the method proposed by Hu and Jacobi (1998) gave the best prediction of the present departure-site spacing database. Pronounced sheet contractions were observed, reaching up to 2/3 of the initial sheet length. The reduction of the wet length was found to be substantial also for the column and droplet flow modes. Notable effects of hysteresis on the film flow contraction when changing the film flow rate were observed. In general, the longitudinal film flow contraction increases with increasing tube diameter and intertube distance.

#### **5. Acknowledgement**

The author gratefully acknowledges support through a post-doctoral assistantship given by the National Council for Scientific and Technological Development of the Ministry of Science and Technology of Brazil, CNPq. The support through the Air Conditioning and Refrigeration Center (ACRC) at the University of Illinois, where the experimental campaign was realized, and the precious advises of Prof. Anthony M. Jacobi, who was the coordinator at the ACRC of the research team that the author joined for his post-doctoral research, are also recognized and gratefully acknowledged.

#### **6. References**

- Armbruster, R. and Mitrovic, J., 1994, "Patterns of falling film flow over horizontal smooth tubes", Proceedings of the 10th Int. Heat Transfer Conference, Vol. 3, Brighton, U.K., pp. 275-280.
- Armbruster, R. and Mitrovic, J., 1995, "Heat transfer in falling film on a horizontal tube", Proceedings of the 1995 National Heat Transfer Conference – vol. 12, ASME HTD-vol. 314, Portland, pp. 13-21.
- Bellman, R. and Pennington, R. H., 1954, "Effects of surface tension and viscosity on Taylor instability", Q. Appl. Math., Vol. 12, pp. 151–161.
- Ganić, E. N. and Roppo, M. N., 1980, "An experimental study of falling liquid film breakdown on a horizontal cylinder during heat transfer", J. Heat Transfer, Vol. 102, pp. 342-346.
- Habert, M., Ribatski, G. and Thome, J. R., 2006, "Experimental study on falling film flow pattern map and intercolumn distance with R236fa", Proceedings of the 6th International Conference on Boiling Heat Transfer, Spoleto, Italy.
- Honda, H., Nozu, S. and Takeda, Y., 1987, "Flow characteristics of condensate on a vertical column of horizontal low finned tubes", Proceedings of the ASME-JSME Thermal Engineering Joint Conference, Vol. 1, Honolulu, USA, pp. 517–524.
- Hu, X. and Jacobi, A. M., 1996, "The intertube falling film, part 1: Flow characteristics, mode transitions, and hysteresis", J. Heat Transfer, Vol. 118, pp. 616-625, 1996.
- Hu, X. and Jacobi, A. M., 1998, "Departure-site spacing for liquid droplets and jets falling between horizontal circular tubes", Exp. Thermal Fluid Science, Vol. 16, pp. 322-331.
- Mitrovic, J., 1986, "Influence of tube spacing and flow rate on heat transfer from a horizontal tube to a falling liquid film", Proceedings of the 8th Int. Heat Transfer Conference, Vol. 4, San Francisco, U.S.A, pp. 1949-1956.
- Ribatski, G. and Jacobi, A. M., 2005, "Falling-film evaporation on horizontal tubes—a critical review", Int. J. Refrig., Vol. 28, pp. 635-653.
- Ribatski, G. and Thome, J. R., 2005, "A visual study of R134a falling film evaporation on enhanced and plain tubes", Proceedings of the 5th International Symposium on Multiphase Flow, Heat Mass Transfer and Energy Conversion, Xi'an, China.
- Ribatski, G. and Thome, J. R., 2006, "Experimental study on the onset of local dryout in a evaporating falling film on horizontal plain tubes", Exp. Thermal and Fluid Sciences, in press.
- Roques, J. F., Gstoehl, D. and Thome, J. R., 2002, "Falling film transitions on plain and enhanced tubes", J. Heat Transfer, Vol. 124, pp. 491-499.
- Wei, Y. and Jacobi, A. M., 2002, "Vapor-shear, geometric, and bundledepth effects on the intertube falling-film modes", Proceedings of the First International Conference on Heat Transfer, Fluid Mechanics, and Thermodynamics, Vol. 1, Kruger National Park, South Africa, pp. 40–46.
- Yung, D., Lorenz, J. J. and Ganić, E. N., 1980, "Vapor/liquid interaction and entrainment in falling film evaporators", J. Heat Transfer, Vol. 77, pp. 69-73.

#### **7. Copyright Notice**

The author is the only responsible for the printed material included in his paper.